Journal for Technology and Science
Homepage : https://journal.antispublisher.com/index.php/IPTEKS/index
Email : admin@antispublisher.com

e-ISSN : 3047-4337
JOTECH, Vol. 3, No. 3, July 2026
Page 116-124

The Use of Graphene and Smart Coatings to Protect Surfaces from Corrosion

Ahmed A. Qanbar
Collage of Education – Tuz Khurmatu, Tikrit University, Salah Al-Din, Iraq

DOI : https://doi.org/10.61796/ipteks.v3i3.558

Sections Info

Article history:
Submitted: May 17, 2026
Final Revised: June 12, 2026
Accepted: July 07, 2026
Published: August 07, 2026

Keywords:
graphene few-layer
HDI
graphene nanomaterials
GNS
epoxy resin
self-propagation

ABSTRACT

Objective: *Coatings that utilize graphene nanomaterials are considered one of the most efficient materials for corrosion prevention of metals. Unfortunately, the usage of these coatings is not commercially feasible since the process of synthesis is very expensive due to imperfection in the process itself.* ***Method:*** *In this regard, few-layer graphene nanomaterials that were synthesized using the process of self-propagation of high-temperature synthesis were used to create coatings. In a salt spray chamber, the effectiveness of these coatings in preventing metal from corroding was examined.* ***Results:*** *It has been demonstrated that the resulting coatings are far more effective than polymeric coatings, which are mostly composed of epoxy resin, at preventing corrosion on steel surfaces.* ***Novelty:*** *A few-layer graphene particle-based coating hypothesis with excellent efficiency was put fortacross both AWS and Azure environments using the Cloud Data Center Workload Dataset.*

INTRODUCTION

Humanity has struggled with rust ever since humans began actively using metal thousands of years ago. Using different coatings is one of the most efficient ways to stop corrosion [1]. Metals (zinc or lead) [2-4], polymers [5-9], and ceramics [10, 11] are some of the materials that are utilized as the foundation for coating. Nevertheless, corrosion remains an issue in modern times despite the wide range of anticorrosion coatings. Different estimates place the annual economic damage caused by corrosion worldwide at much to 2.5 trillion US dollars [12]. As a result, scientists are still searching for novel materials and methods to create superior coatings. Materials with no more than ten graphene layers are known as Graphene Nano Structures (GNS) [13]. GNS has a "barrier effect" because the graphite structure is very tiny due to the modest size of the carbon hexagon. Water and oxygen molecules cannot flow through GNS in this manner, which leads to corrosion [14]. Due to this characteristic, GNS are frequently utilized in the production of anticorrosive coatings [15–17], either on their own or as a component of polymer composite coatings [18,19]. However, the widespread use of GNS coatings was not yet achieved, despite several trials demonstrating its effectiveness in preventing corrosion processes [20,21]. In actuality, GNS coatings are not widely produced due to their relatively expensive cost. It is brought on by shortcomings in both "top down" [24] and "bottom up" [22, 23] GNS synthesis methods. This method cannot be utilized to produce high-quality, reasonably priced GNS on a big scale. Reviews [20,25,26] showed that the presence of different flaws has a significant impact on the barrier characteristics of GNS and, consequently, on their anti-corrosive capabilities. They also revealed issues with the current GNS synthesis techniques. Because of this, the high throughput

method—which enables us to synthesis huge quantities of high-quality, reasonably priced GNS—is necessary for the use of GNS as an anti-corrosive coating. To address this issue, we demonstrated in our earlier paper [27] that the SHS approach may be used to synthesize few-layer graphene (FLG, up to 5 layers) from cyclic biopolymers [28]. It has been demonstrated in the context of our earlier research that the synthesized FLG may effectively be added to polymer composite materials to improve their mechanical, thermophysical, and tribological characteristics [30, 31]. Because of their chemical bonding, this study demonstrates the first use of FLG particles generated utilizing the SHS approach for coatings manufacture. Additionally, this study offers first findings about the effectiveness of FLG particles for the anticorrosion protection of metals.

METHODOLOGY

Material of few-layer graphene Coatings

Few layer graphene (FLG), which has five layers or less, was used to create the coating material. In a tumbler mixer, glucose and ammonium nitrate were combined in a 1:1 weight ratio to create the FLG. After that, this combination was put in a reactor and heated to 250 C^o, the temperature needed to start the SHS reaction. Gas production was employed to signal the start of the reaction, and its termination indicated its end. After the SHS reaction was finished, the powder was cleaned with deionized water and dried at 110°C in an oven until it became a stable mass. Reference [28] provides a comprehensive description of the FLG synthesis process. The synthesized FLG was shown to be free of Stone-Wales flaws using a chemical approach for counting them [29].

Manufacturing method and process

The GNS contains many functional groups, including –OH and –COOH [32, 33]. Functional groups are also present on the surface of FLG, which is the raw material utilized to create the coating. The FLG particles can now be chemically bonded via functional groups. Figure 1 shows a schematic representation of the coating preparation procedure.

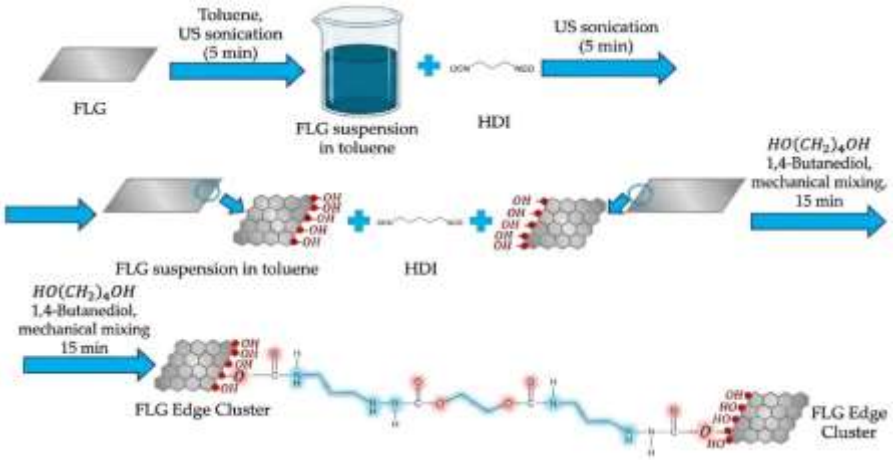

Figure 1. Schematic diagram of the synthesis of the coating material using chemical bonding of FLG.

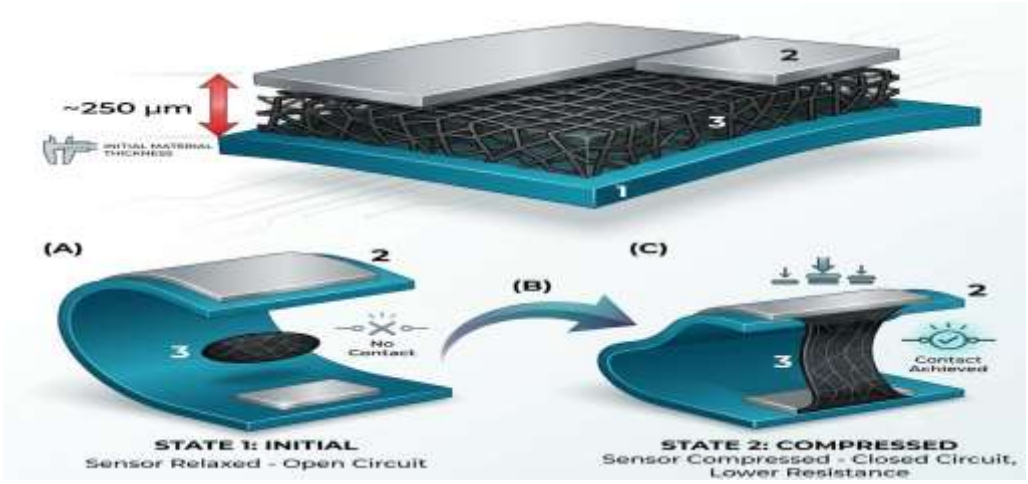

Figure 2. The mechanics of paint and how it is applied.

molecules The substrate materials were steel sheets (Grade St-08ps) measuring 80 mm × 200 mm × 2 mm (length × width × thickness). Hexamethylene isosinate was used as a cross-linking agent, and the backbone of the chain was ethylene glycol. Because it contains active groups (NCO), HDI is an aliphatic isocyanate that is frequently utilized as a cross-linking agent in polymer chemistry. Figure 1 depicts the scheme of responses.To prepare the coating, FLG dispersion was sonicated for five minutes in toluene (reagent grade, Sigma-Aldrich). After then, the HDI was added to the FLG dispersion and sonicated for a further five minutes. The necessary quantity of ethylene glycol, a chain extender, was then combined with the toluene-HDI-FLG dispersion.Using an applicator with a steel roller and a 300 µm space between them, the produced dispersion was applied to the steel surface. Fig. 2 illustrates the coating application procedure. The coatings were then dried for 36 hours at 110 °C to remove all of the toluene and in the fig.3. A sample of an FLG.

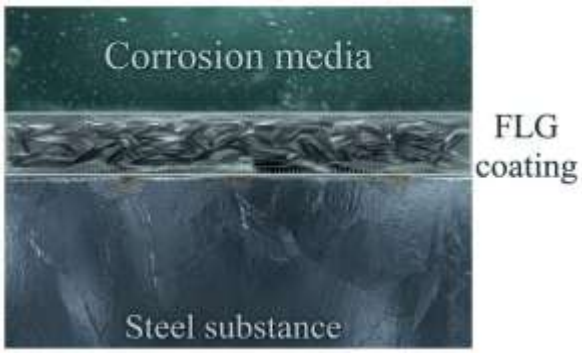

Figure 3. A sample of an FLG-particle-based composite coating applied to a steel substrate.

Characterisation of graphene and graphene-based coatings

The morphological characteristics of the synthesised material were studied, taking into account the particle shape. Five minutes after ultrasonic treatment, Fourier transform infrared spectroscopy was performed, followed by Raman spectroscopy measurements using an Ntegra Spectra Raman microscope, featuring a 600 grooves/mm grating, a 100× magnification lens, and a laser wavelength of 532 nanometres. To prevent the material from overheating due to the laser beam, the laser power density was kept below 50 microwatts per square micrometre. The data show the average spectral values, collected from several locations on randomly selected samples. Coating thickness was measured using a micrometre, and the ASTM D3359 method was used to assess the adhesion of the coating to the steel substrate using a QFH-A cross-cut adhesion tester. The water contact angle was measured using the single-drop method with a single drop of deionised water with a volume of 10 microlitres. The ASTM B117 method was used to assess the corrosion resistance of the coatings using an HSL-60 T salt spray tester, and an aqueous solution with a pH of 6.5 containing 5% by weight of sodium chloride (NaCl) was used as the corrosive environment. Prior to the start of the test, scratches 100 mm long and 0.4 mm wide were made on the surfaces of the coated materials. The test duration was 48 hours. The electrical resistance of the FLG coating was measured using a multimeter.

RESULTS AND DISCUSSION

The FLG particles used in coating synthesis are shown in electron micrographs in Figure 4(a). The generated FLG particles had lateral sizes ranging from many tens of micrometers, as seen in the image. To get a quantifiable distribution, laser diffraction analysis was employed. In Figure 4(a), the results are shown.

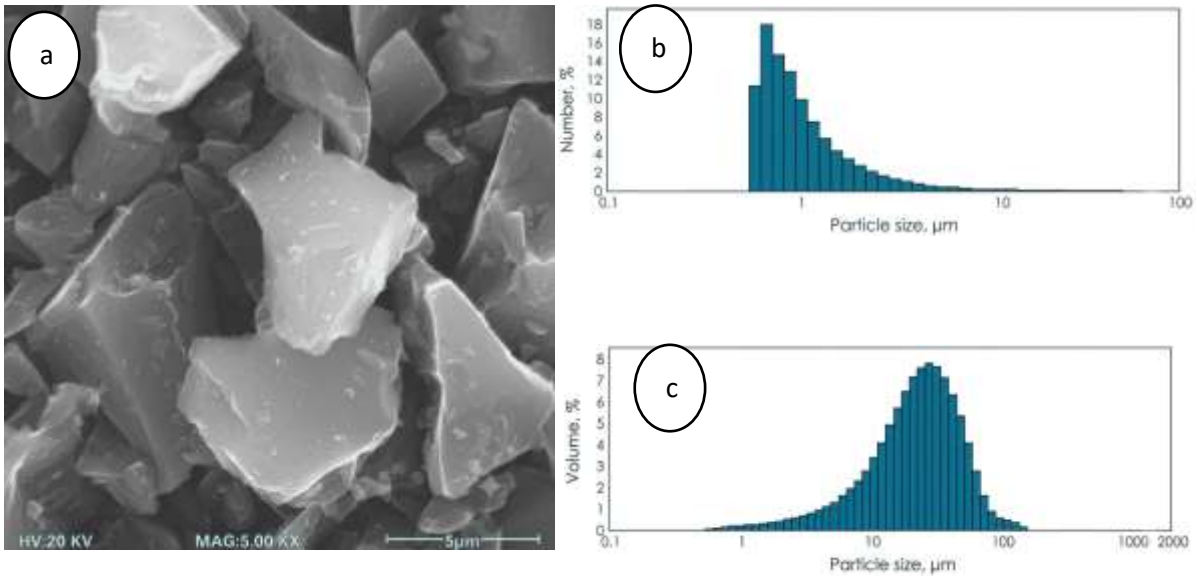

Figure 4. (a) Examination of FLG particles using a scanning electron microscope, (b) Average nanoparticle size distribution, (c) Average number of particles.

The FLG powder sample does contain particles with lateral dimensions in the tens of micrometers range, as seen in Figure 4a, although their percentage is incredibly small.

The particle size distribution graph in Figure 4b shows that most of the particles were between 0.5 and 1 µm in diameter. The average thickness of the epoxy reference film is 245 ∓ 35 µm, which is similar to the 260 ∓ 30 µm of the FLG film. To understand the FLG coating's internal structure, the SEM technique was employed. As a result, the chemical cross-linking of FLG particles created the side-view image on the film.

The C=C vibrations at 1558 cm^{-1} and the C–O vibrations at 1224 cm^{-1} are two broad bands in the FT-IR spectra of pure few-layer graphene, as shown in Figure 5. It is believed that the various ethers and alcohols formed during the uncontrolled SHS process are responsible for the broadening of the bands in this case [36]. However, the FT-IR spectrum of the chemically cross-linked FLG coating shown in Figure (5) exhibits a number of characteristic bands indicative of the formation of new chemical bonds; consequently, the appearance of these vibrational bands indicates that the FLG particles have successfully undergone the chemical cross-linking process. It can be observed that the relatively low intensities of the N–H and C=O bands overlap with the broad band of C=C vibrations in the graphene structure.

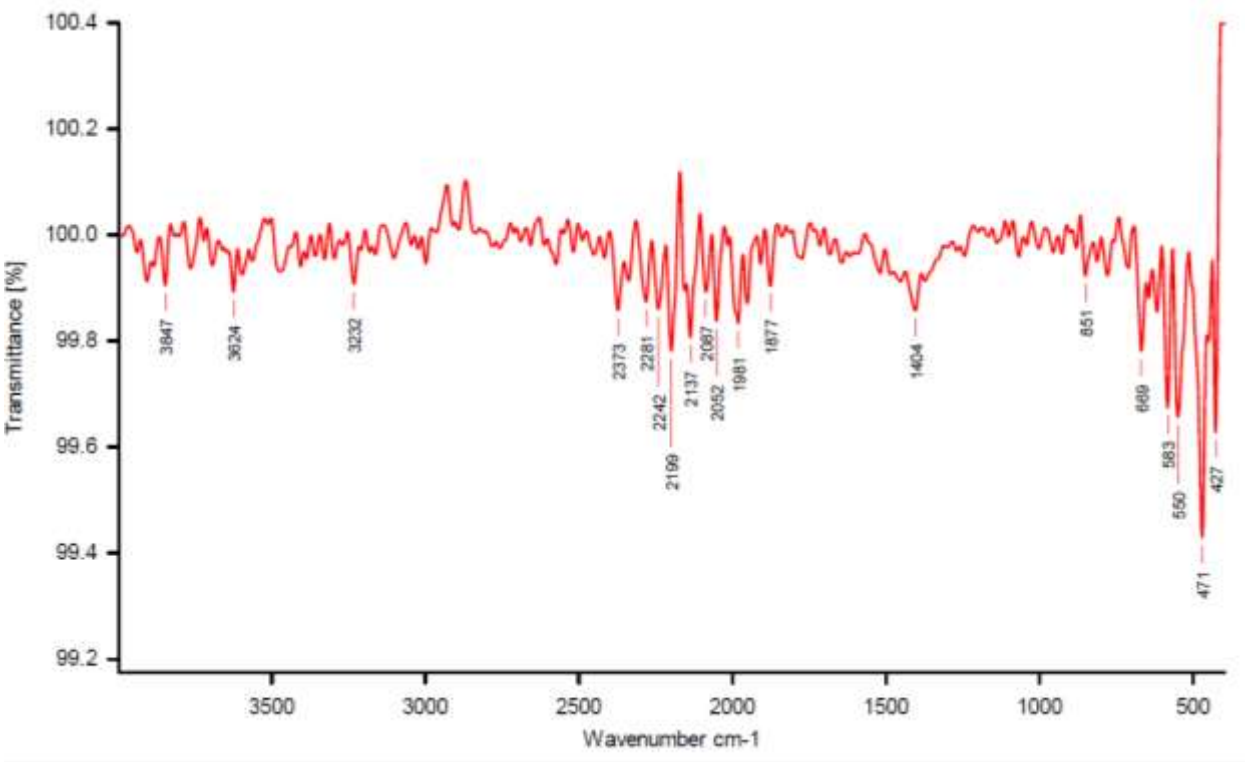

Figure 5. FTIR spectrum of the chemically synthesized FLG layer.

Figure 6 [38] shows that both samples contain characteristic peaks D and G that correspond to the Raman spectra of graphene materials. Peak G (~1580 cm-1) is associated with the vibration of sp2 hybridized carbon atoms in the graphite lattice. However, peak D (~1350 cm-1) arises due to structural defects in the graphene structure [39]. The number of structural faults may be estimated using the ID/IG ratio, where ID and IG represent the intensity of the D and G peaks, respectively.

It is 0.75 for the cross-linked coating and 0.94 for the pure FLG powder sample. A decline in the ID/IG ratio might be a sign of a lower defect density in the sample. The D peak is believed to be primarily caused by the presence of graphene sheet edges that terminate with various functional groups, such as –OH and –COOH [40]. Thus, we suggest that during the cross-linking process, the same functional groups may somehow "stitch" the edges.

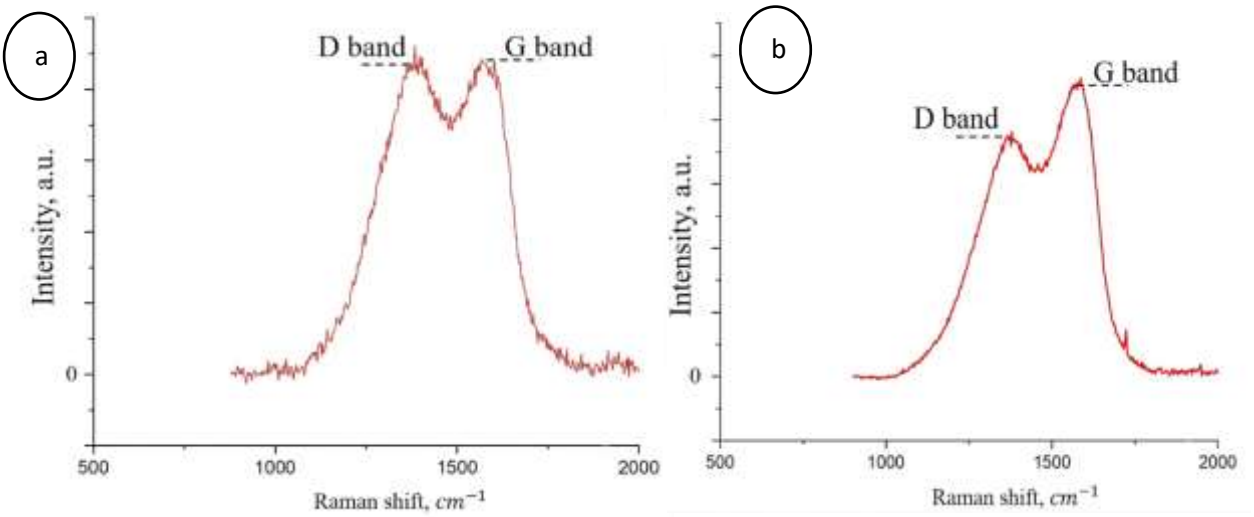

Figure 6. Raman spectra of the original FLG (a) and the coating formed by the chemical bonding.

of molecules of graphene few-layer (b). Such effectiveness is ensured by the synergy between the special qualities of the graphene few-layer produced using SHS technology and the peculiarities of the microstructure of the cross-linked film. First, the lack of Stone-Wales defects [29] guarantees the FLG flakes' low intrinsic permeability to corrosive media (such water and ions), which is a key advantage. Second, the film has a high electrical resistance of over 20 MΩ. It is connected to the chaotic microstructure, cross-linking structure, and edge functional groups. By inhibiting the development of micro-galvanic cells at the graphene-metal interface, this low conductivity reduces a major source of corrosion in conductive graphene-based composites. Third, the actual structure of the coating plays an important part. The corrosive medium's path into the structure is complicated since the film is composed of many randomly oriented FLG aggregates and particles. Because the FLG flakes overlap, the corrosive medium will still need to come into contact with non-defective areas of the underlying flakes even if a flake's fault is avoided. This will delay the commencement of corrosion.

CONCLUSION

Fundamental Finding: This study is the first to investigate the anti-corrosive properties of chemically cross-linked few-layer graphene particle coatings. The findings demonstrate that these coatings provide substantially greater corrosion resistance than conventional epoxy resin coatings of the same thickness due to the enhanced barrier

effect created by multiple graphene layers that effectively cover structural defects. **Implication:** The results suggest that few-layer graphene coatings produced using the self-propagating high-temperature synthesis (SHS) process offer a cost-effective and scalable solution for high-performance corrosion protection, supporting their potential application in industrial metal coating technologies. **Limitation:** The study primarily evaluates corrosion resistance through neutral salt spray testing and does not quantitatively assess the coatings' electrochemical performance or compare graphene coatings with different chemical lattice structures and defect characteristics. **Future Research:** Future research should compare graphene nanomaterial coatings with varying chemical lattice structures and defect densities to clarify the mechanisms underlying corrosion resistance, while employing electrochemical testing to quantitatively evaluate their long-term anti-corrosive performance.

REFERENCES

[1] Alavi, A. and R. A. Cottis. 1987. The determination of pH, potential and chloride concentration in corroding crevices on 304 stainless steel and 7475 aluminium alloy. Corrosion Science 27: 443–451.

[2] Bhaskaran, R., N. Palaniswamy, N. S. Rengaswamy and M. Jayachandran. 2005. Global cost of corrosion—a historical review. pp. 621–628. *In*: Cramer, S.D. and B.S. Covino (eds.). Corrosion: Materials, ASM International.

[3] Becquerel, A. C. 1834. Experimental treatise on electricity and magnetism, and their relations with natural phenomena. Vol. Didot.

[4] De La Rive, A. 1830. "N"ote relatire a 1'action qu'exerce sur le zinc 1'acide sulfuriąue etendu d'eau. Ann. Chira. Phys. (2. ser.), 43: 425–440.

[5] Tweney, R. D. 1992. Inventing the field: Michael Faraday and the creative of electromagnetic field theory. Inventive Minds: Creativity in Technology 31.

[6] Bibliography of the metals of the platinum group: Platinum, palladium, iridium, rhodium, osmium, ruthenium, 1748–1917, 1919.

[7] Gaiser, L. and K. E. Heusler. 1970. Die kinetik der zinkelektrode in zinkperchloratlösungen, Electrochimica Acta 15: 161–171.

[8] Heusler, K. E. and L. Gaiser. 1970. The mechanism of the cadmium electrode. Journal of the Electrochemical Society 117: 762.

[9] 'M. Bockris, J. O. 1989. Spectroscopic observations on the nature of passivity. Corrosion Science 29: 291–312.

[10] Wu, X. Q., Y. S. Yang, Q. Zhan and Z. Q. Hu. 1998. Structure degradation of 25Cr35Ni heat-resistant tube associated with surface coking and internal carburization. Journal of Materials Engineering and Performance 7: 667–672.

[11] El Azhar, M., M. Traisnel, B. Mernari, L. Gengembre, F. Bentiss and M. Lagrenée. 2002. Electrochemical and XPS studies of 2,5-bis(n-pyridyl)-1,3,4-thiadiazoles adsorption on mild steel in perchloric acid solution. Applied Surface Science 185: 197–205.

[12] Hermas, A. A., M. Nakayama and K. Ogura. 2005. Formation of stable passive film on stainless steel by electrochemical deposition of polypyrrole, Electrochimica Acta 50: 3640–3647.

[13] Rajendran, A. 2011. Isolation, characterization, pharmacological and corrosion inhibition studies of flavonoids obtained from Nerium oleander and Tecoma stans. International Journal of PharmTech Research 3: 1005–1013.

[14] Yeh, J. -M., C. -L. Chen, Y. -C. Chen, C. -Y. Ma, K. -R. Lee, Y. Wei and S. Li. 2002. Enhancement of corrosion protection effect of poly(o-ethoxyaniline) via the formation of poly(o-ethoxyaniline)– clay nanocomposite materials. Polymer 43: 2729–2736.
[15] Woodruff, D. P. 2016. Modern Techniques of Surface Science. Cambridge University Press, Cambridge.
[16] Migahed, M. A., M. Abd-El-Raouf, A. M. Al-Sabagh and H. M. Abd-El-Bary. 2005. Effectiveness of some non ionic surfactants as corrosion inhibitors for carbon steel pipelines in oil fields. Electrochimica Acta 50: 4683–4689.
[17] Ellmer, K. 2000. Magnetron sputtering of transparent conductive zinc oxide: relation between the sputtering parameters and the electronic properties. Journal of Physics D: Applied Physics 33: R17–R32.
[18] Quraishi, M. A., J. Rawat and M. Ajmal. 2000. Dithiobiurets: a novel class of acid corrosion inhibitors for mild steel. Journal of Applied Electrochemistry 30: 745–751.
[19] Zhang, X., W. G. Sloof, A. Hovestad, E. P. M. van Westing, H. Terryn and J. H. W. de Wit. 2005. Characterization of chromate conversion coatings on zinc using XPS and SKPFM. Surface and Coatings Technology 197: 168–176.
[20] Amalraj, A., M. Sundaravadivelu, A. P. Regis and S. Rajendran. 2001. Corrosion inhibitor for carbon steel in ground water. Bulletin of Electrochemistry 17: 179–182.
[21] Ravichandran, R., S. Nanjundan and N. Rajendran. 2004. Effect of benzotriazole derivatives on the corrosion of brass in NaCl solutions. Applied Surface Science 236: 241–250.
[22] Alves, V., A. M. C. Paquim, A. Cavaleiro and C. Brett. 2005. The nanostructure and microstructure of steels: Electrochemical Tafel behaviour and atomic force microscopy. Corrosion Science — CORROS SCI. 47: 2871–2882.
[23] Blunt, J. W., B. R. Copp, R. A. Keyzers, M. H. G. Munro and M. R. Prinsep. 2016. Marine natural products. Natural Product Reports 33: 382–431.
[24] Adey, R. A., S. M. Niku, C. A. Brebbia and J. Finnegan. 1986. Computer aided design of cathodic protection systems. Applied Ocean Research 8: 209–222.
[25] Kendig, M. W., E. M. Meyer, G. Lindberg and F. Mansfeld. 1983. A computer analysis of electrochemical impedance data. Corrosion Science 23: 1007–1015.
[26] Goldie, B. P. and J. J. McCarroll. 1984. Inhibiting corrosion in aqueous systems. US Patent.
[27] Jacobson, G. 2016. International Measures of Prevention, Application, and Economics of Corrosion Technologies Study. Houston, USA.
[28] Evans, U. R. 1981. An Introduction to Metallic Corrosion. 3rd Ed., Edward Arnold, London.
[29] Whitney, W. R. 1903. The corrosion of iron. J. Am. Chem. Soc. 25: 394–406.
[30] Walker, W. 1913. The corrosion of iron and steel. J. Ind. Eng. Chem. 5: 444–445.
[31] Tremont, R., H. de Jesús-Cardona, J. García-Orozco, R. J. Castro and C. R. Cabrera. 2000. 3-Mercaptopropyltrimethoxysilane as a Cu corrosion inhibitor in KCl solution. Journal of Applied Electrochemistry 30: 737–743.
[32] Kucera, V. (ed.). 1988. The Effect of Acidification on Corrosion of Structures and Cultural Property. John Wiley & Sons Ltd.
[33] Lynes, W. 1951. Some historical developments relating to corrosion. J. Electrochem. Soc. 98: 3C.
[34] Yamashita, M., H. Konishi, T. Kozakura, J. Mizuki and H. Uchida. 2005. *In situ* observation of initial rust formation process on carbon steel under Na_2SO_4 and NaCl solution films with wet/dry cycles using synchrotron radiation X-rays. Corrosion Science 47: 2492–2498.
[35] Leyerzapf, H. 1985. Zur Bedeutung und Geschichte des Wortes "Korrosion". Werkstoffe und Korrosion 88–96.
[36] Al-Otaibi, M. S., A. M. Al-Mayouf, M. Khan, A. A. Mousa, S. A. Al-Mazroa and H. Z. Alkhathlan. 2014. Corrosion inhibitory action of some plant extracts on the corrosion of mild steel in acidic media. Arabian Journal of Chemistry 7: 340–346.
[36] Ebenso, E. E., M. M. Kabanda, T. Arslan, M. Saracoglu, F. Kandemirli, L. C. [37]Murulana, A. K. Singh, S. K. Shukla, B. Hammouti, K. F. Khaled and M. A. Quraishi. 2012. Quantum

chemical investigations on quinoline derivatives as effective corrosion inhibitors for mild steel in acidic medium. International Journal of Electrochemical Science 5643–5676.
[38] Fiala, A., A. Chibani, A. Darchen, A. Boulkamh and K. Djebbar. 2007. Investigations of the inhibition of copper corrosion in nitric acid solutions by ketene dithioacetal derivatives. Applied Surface Science 253: 9347–9356.
[39] Peter, A., I. B. Obot and S. K. Sharma. 2015. Use of natural gums as green corrosion inhibitors: an overview. Int. J. Ind. Chem. 6: 153–164.
[40] Jerkiewicz, G. 1995. Examination of factors influencing promotion of H absorption into metals by site-blocking elements. J. Electrochem. Soc. 142: 3755.

Ahmed A. Qanbar
Collage of Education – Tuz Khurmatu, Tikrit University, Salah Al-Din, Iraq
Email : ahmed.abd.tuz@tu.edu.iq